Comparison of 2-D and 3-D slope stability analyses for unsaturated soil slopes

Lulu Zhang
State Key Laboratory of Ocean Engineering, Shanghai Jiaotong University Shanghai, China
Murray D. Fredlund
SoilVision Systems Ltd., Saskatoon, SK., Canada
Delwyn G. Fredlund
Golder Associates Ltd., Saskatoon, SK., Canada
Haihua Lu
SoilVision Systems Ltd., Saskatoon, SK., Canada

ABSTRACT
Most past comparative studies between 2-D and 3-D stability analyses have ignored the effect of negative pore-water pressures (i.e., matric suctions) in the soil zone above the groundwater table. In this paper, a comparison is made between 2-D and 3-D slope stability analyses on soil slopes where a portion of the soil profile has matric suctions. The factors of safety on simple geometry slopes, complex geometry slopes which have two intersecting slope surfaces, are investigated under various shear strength parameters and groundwater conditions. For simple slopes with a low slope angle, the difference in factor of safety between a 2-D and 3-D slope stability analysis, (i.e., $\Delta F_s/F_{s2\text{-}D}$), generally ranges from 9% to 16% when ϕ^b is equal to 15 degree. The value of $\Delta Fs/F_{s2\text{-}D}$ for a steep, simple slope is generally larger than that of a low angle, simple slope. The difference between a 2-D and 3-D stability analysis was most pronounced for concave geometries where a portion of the soil profile contained unsaturated soils. The values of $\Delta F_s/F_{s2\text{-}D}$ for concave slopes with a corner angle between 180 to 270 degrees can be as large as 20 to 59% when ϕ^b is equal to 15 degree. The case history of the high-wall stability failure at the Poplar River coal mine was back-calculated to illustrate the effect of unsaturated zone on back-analyzed shear strength parameters.

RÉSUMÉ
La plupart des études comparatives entre les deux dernières 2-D et de la stabilité 3-D analyses ont ignoré l'effet de pressions interstitielles négatives (succions matricielles) dans la zone de sol au-dessus de la nappe phréatique . Dans cet article, une comparaison est faite entre 2-D et 3-D stabilité de la pente des analyses sur les pentes du sol où une partie du profil de sol a succions matricielles. Les facteurs de sécurité sur la géométrie des pentes simples, la géométrie des pentes complexes qui ont deux surfaces de pente qui se croisent, sont étudiées sous différents paramètres de résistance au cisaillement et les eaux souterraines. Pour les pentes simples avec un angle d'inclinaison faible, la différence de coefficient de sécurité entre une analyse 2-D et 3-D stabilité des talus, (ΔFs/Fs2-D), est généralement comprise entre 9% et 16% lorsque ϕ^b est égal à 15 degrés. La valeur de ΔFs/Fs2-D pour, une pente raide simple est généralement plus grande que celle d'un faible angle, pente simple. La différence entre un 2-D et 3-D analyse de stabilité a été plus prononcée pour les géométries concaves où une partie du profil de sol contenait des sols non saturés. Les valeurs de ΔFs/Fs2-D pour pentes concaves avec un angle de coin entre 180 270 degrés peuvent être aussi grand que 20 à 59% quand ϕ^b est égal à 15 degrés. L'histoire de l'échec de la stabilité à haute paroi de la mine de charbon de la rivière Poplar cas était de retour-calculé pour illustrer l'effet de la zone non saturée sur les paramètres de sauvegarde analysé la résistance au cisaillement .

1 INTRODUCTION

Two-dimensional (2-D) limit equilibrium methods (LEM) of slope stability analysis remain the most common method of analysis in slope engineering practice. However, most engineering problems have three-dimensional characteristics that cannot be taken into account by conventional two-dimensional plane strain representations. Most natural landslides are three-dimensional in character and the geometries are too complex to be accurately modeled using a two-dimensional representation of the geometry. Other engineering problems which are inherently three-dimensional include mining pit, tailings and mine rock piles, deep excavation with corners, earth and rock fill dam or levees, earth storage, and municipal solid waste slope (Fredlund et al. 2012b; Yu et al. 2005). A three-dimensional (3-D) analysis can accommodate variations in geometry, pore-water pressures, and material properties across a site.

Three-dimensional methods of slope stability analysis are usually extensions of conventional two-dimensional approaches (Hovland 1977; Chen and Chameau 1982; Leshchinsky and Baker 1986; Zhang 1988, Hungr et al. 1987; Lam and Fredlund 1993; Chen et al. 2001; Cheng and Yip 2007; Zheng 2012). Kalatehjari and Ali (2013) undertook an extensive review of 3-D analyses. It is generally assumed that a 2-D slope stability analysis provides a more conservative estimate of a 3-D slope

stability problem, provided that 2-D stability analysis is calculated for the most critical two-dimensional section (Duncan 1996). The difference in the factors of safety of a slope between a 2-D and 3-D analysis is generally less than 15% for simple slope geometries. Adriano et al. (2008) found that differences in the critical factor of safety of 15% to 50% between 3-D and 2-D stability analysis based on finite element modeling for concave and convex slopes. There are some reported differences in factor of safety that are greater than 50% (Chen and Chameau, 1982; Leshchinsky and Barker, 1986). The differences were mainly due to the shape of critical slip surfaces. Leshchinsky et al., (1992), Lam and Fredlund (1993) and Stark and Eid (1998) presented case studies which demonstrated that ignoring 3-D effect may lead to an over-estimation of the *in situ* shear strength. A 3-D analysis was recommended for the back-analysis of slope failures so the back-calculated shear strength would reflect the 3-D end effects.

Most previous studies comparing 2-D and 3-D stability analysis ignore the effect of negative pore-water pressures (i.e., matric suctions) in the soil zone above the groundwater table (Leong and Rahardjo, 2012). In this paper, a comparison study is reported between 2-D and 3-D slope stability analysis for soil slopes where a portion of the soil profile has matric suctions.

2 THREE-DIMENSIONAL GENERAL LIMIT EQUILIBRIUM METHOD FOR SLOPE STABILITY ANALYSIS

Lam and Fredlund (1993) proposed a 3-D method as an extension of the general 2-D limit equilibrium method of Fredlund and Krahn (1977). A rotational surface with a single direction of movement was assumed for the slip surface. The basic definition of these inter-column force functions was similar to that proposed by Morgenstern and Price (1965) including five relationships between normal and shear inter-column forces. Lam and Fredlund (1993) used the finite element analysis results to compute inter-column forces for typical slopes and suggested that it was reasonable to consider only the *E/X* and *V/P* functions rather than all five functions when performing a three-dimensional analysis. The free-body diagram of a column for the general 3-D limit equilibrium method with simplified inter-column forces is presented in Fig. 1. The forces are defined as follows: *W* is weight of the column; *N* is the normal force at the base of each column; S_m is the shear force mobilized at the base of each column; E_L, E_R are inter-column normal forces on YZ plane, where the subscripts L and R represents the left side and right side planes, respectively; P_L, P_R are the inter-column normal forces on XZ plane; X_L, X_R are the inter-column vertical shear force on YZ plane; V_L, V_R are the inter-column vertical shear force on XZ plane; α_x and α_y are the inclination angles of the column base in the X and Y directions, respectively; θ_x, θ_y, θ_z are direction angles of the normal force *N* at the column base along *X, Y, Z* directions, respectively.

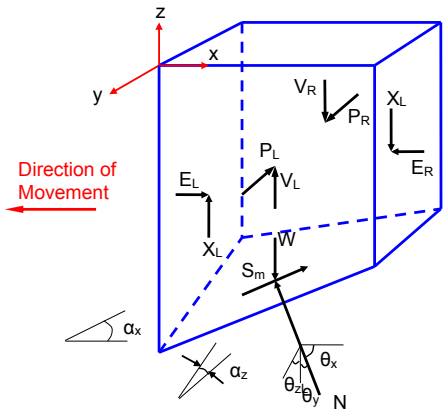

Figure 1. Free body diagram of a column using simplified assumptions for inter-column forces (modified from Lam & Fredlund, 1993).

The overall factor of safety value was determined that simultaneously satisfied moment and force equilibrium. Moment equilibrium was taken with respect to a common axis of rotation above the entire failure mass. The factor of safety with respect to moment equilibrium, F_m, can be derived by summing the moment of all the forces over the entire sliding mass about the axis of rotation (Lam and Fredlund 1993; Fredlund et al., 2012a):

$$F_m = \frac{\sum\left[\left(c'A + (N-U)\tan\phi'\right)\left(\cos\alpha_x d_y + \sin\alpha_x d_x\right)\right]}{\sum\left(N\cos\theta_x d_y + N\cos\theta_y d_x + W d_x\right)} \quad [1]$$

The factor of safety with respect to force equilibrium, F_f, in 3-D is derived by summing forces in the x-direction over the entire failed mass (Lam and Fredlund, 1993; Fredlund et al., 2012a):

$$F_f = \frac{\sum\left(c'A + \left(N-U\right)\tan\phi'\right)\cos\alpha_x}{\sum N\cos\theta_x} \quad [2]$$

where *A* is the area of the column base, *c'* is effective cohesion, ϕ' is the effective friction angle, *U* is the pore-water force acting on the base of the column, d_x is the x-moment arm with respect to the axis of moments, d_y is the y-moment arm with respect to the axis of moments. Both the equations for F_m and F_f are non-linear since the normal force *N* in each equation is also a function of the factor of safety. An iterating procedure can be used to solve the moment and force equilibrium factors of safety.
In this study, the slip surface in 3-D slope stability analysis is assumed to be ellipsoidal. The computer software program, *SVSlope* (Fredlund, 2009), which has incorporated a variety of commonly used 3-D limit equilibrium methods of slope analyses, is used to calculate the factors of safety for the example problems.

3 EXAMPLES OF SIMPLE GEOMETRY SLOPES

The factors of safety on simple geometry slopes with a low slope angle and a steep slope angle are first investigated using various selected shear strength parameters and groundwater conditions.

3.1 Stability analysis of a low angle, simple slope

The low angle simple geometry slope is 20 meters high and the slope angle is 30 degree (Fig. 2). Three levels of groundwater table (denoted as GWT #1, #2 and #3) are considered. GWT #1 is a shallow groundwater table which represents the situation where the slope is almost fully saturated. GWT #3 is a deep groundwater table. The maximum difference between the three groundwater levels is approximately 10 m. The pore-water pressure conditions in the slope are assumed to be hydrostatic both above and below the piezometric line.

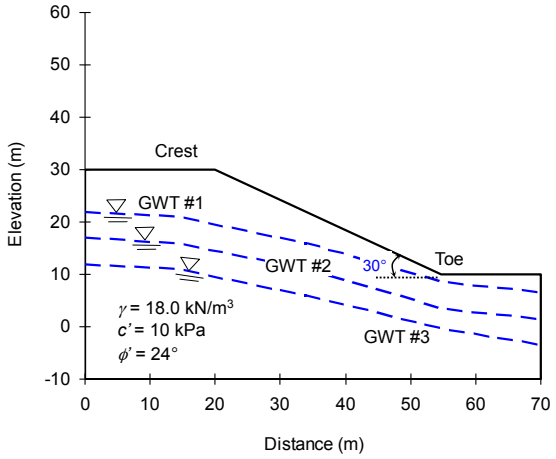

Figure 2. Geometry of a low angle slope geometry along with three levels of the groundwater table.

Assuming the effective shear strength parameters are fixed values (i.e., c' is 10 kPa and ϕ' is 24°), Figure 3 presents the difference in the factor of safety between a 2-D and 3-D slope stability analysis ($\Delta F_s/F_{s2\text{-}D}$), for various ϕ^b values. The factors of safety for both 2-D and 3-D analyses are obtained for critical slip surfaces. Figure 3 shows that the difference of factor of safety between 2-D and 3-D slope stability analysis, $\Delta F_s/F_{s2\text{-}D}$, is increased with the increase of ϕ^b. The increased rate of change in $\Delta F_s/F_{s2\text{-}D}$ is slightly affected by the location of groundwater table. The variation of $\Delta F_s/F_{s2\text{-}D}$ is largest for GWT #2, which is neither the highest nor the lowest groundwater table among the three assumed three ones. For the highest groundwater table (GWT #1), most portion of critical slip surfaces are in the saturated soil zone. The increase of ϕ^b does not contribute much to the increase of $\Delta F_s/F_{s2\text{-}D}$. For the lowest groundwater level (GWT #3), the critical slip surfaces are mainly in the unsaturated zone for ϕ^b increases from zero to 15 degree (62.5% ϕ') and the increased rate of $\Delta F_s/F_{s2\text{-}D}$ is high. However, with the further increase of ϕ^b value, the critical slip surface becomes deeper and the contribution of unsaturated zone to $\Delta F_s/F_{s2\text{-}D}$ is reduced.

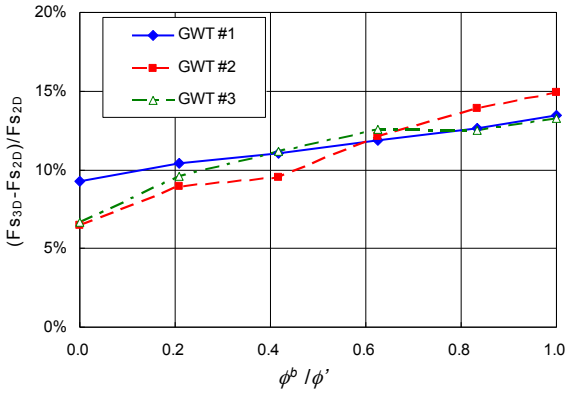

Figure 3. Difference of factor of safety for the low slope geometry with c' = 10 kPa and ϕ' = 24°.

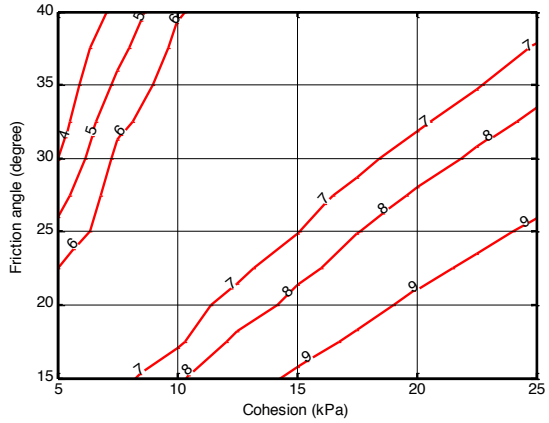

(a) Factor of safety difference when ϕ^b = 0

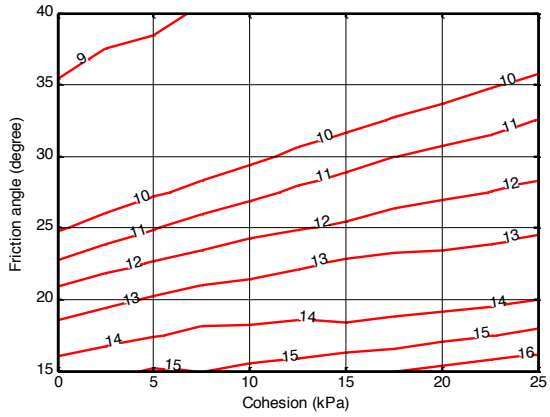

(b) Factor of safety difference when ϕ^b = 15°

Figure 4. Contours of F_s difference, $\Delta F_s/F_{s2D}$ (%) for the low slope geometry (GWT #2): (a) ϕ^b = 0 (b) ϕ^b = 15°.

Figure 4 presents the contours of $\Delta F_s/F_{s2\text{-}D}$ for the low angle, simple slope for various combinations of shear strength parameters. Figure 4(a) and 4(b) show the contours of $\Delta F_s/F_{s2\text{-}D}$ with an assumed ϕ^b value of zero

and 15 degree, respectively. The difference in factor of safety between a 3-D and 2-D analysis monotonically increases with c' and ϕ'. The variation of $\Delta F_s/F_{s2\text{-}D}$ ranges from 4% to 9% when the effect of matric suction is ignored. The variation in $\Delta F_s/F_{s2\text{-}D}$ ranges from 9% to 16% when ϕ^b is 15 degrees.

3.2 Stability analysis of a steep angle, simple slope

The steep slope is 30 meters high and the slope angle is 50 degree (Fig. 5). Three levels of groundwater tables are once again considered. The groundwater table varies from a high level (GWT #1) which exits at the toe of the slope to the level (GWT #3) which is around 18 m below the toe of the slope.

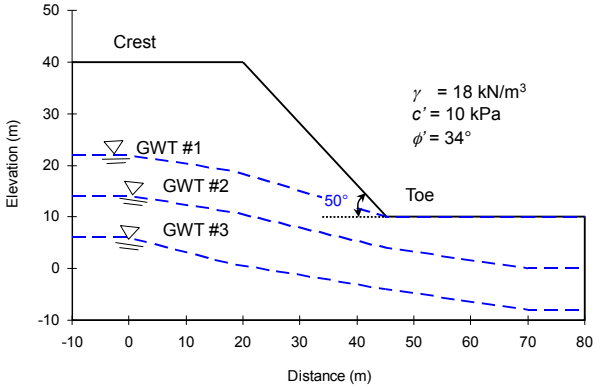

Figure 5. Geometry of a steep angle simple slope geometry and three levels of groundwater table.

Figure 6 presents the difference of factor of safety for various levels of groundwater table with given soil shear strength parameters (i.e., c' is 10 kPa and ϕ' is 34°). For a steep simple slope geometry, the values of $\Delta F_s/F_{s2\text{-}D}$ do not monotonically increase with ϕ^b. This behavior is different from the result for the low angle simple slope.

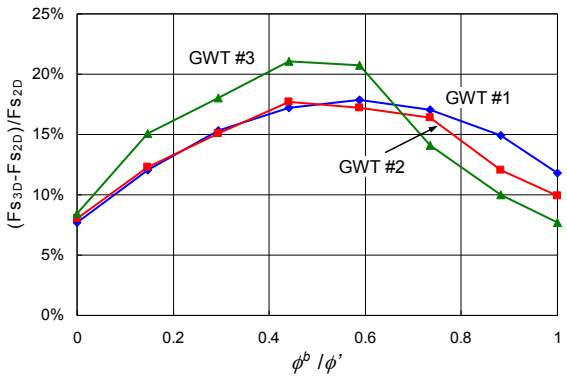

Figure 6. Difference of factor of safety for the steep slope geometry with c' = 10 kPa and ϕ' = 34° with various groundwater tables.

The peak values occur around ϕ^b equal to 40% to 60% of ϕ'. The effect of groundwater table level is more significant for the steep slope than for the low angle slope. This is mainly because the assumed variation in the depth of the groundwater table is much greater for the steep slope than for the low angle slope.

Figure 7 presents the contours of $\Delta F_s/F_{s2\text{-}D}$ for the low angle, simple slope for various combinations of shear strength parameters. The difference in the factor of safety does not monotonically increase with c' and ϕ'. With the omission of ϕ^b (Figure 7a), the variation of $\Delta F_s/F_{s2\text{-}D}$ ranges from 6% to 13%. The values of $\Delta F_s/F_{s2\text{-}D}$ range from 12% to 18% when ϕ^b is assumed to be 15 degrees (Figure 7b). These results are for GWT #2. According to Figure 6, the changes of $\Delta F_s/F_{s2\text{-}D}$ may be greater for the case of the GWT#3 level. Comparing Figure 7 to Figure 4, it can be seen that the difference of factor of safety between a 2-D and 3-D analysis for a steep slope is generally larger than that for a low angle slope. However, for a simple, steep slope, $\Delta F_s/F_{s2\text{-}D}$ does not increase monotonically with the shear strength parameters (i.e., c', ϕ').

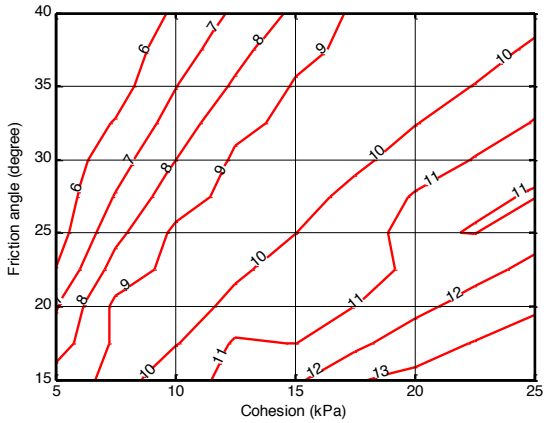

(a) Factor of safety difference when ϕ^b = 0

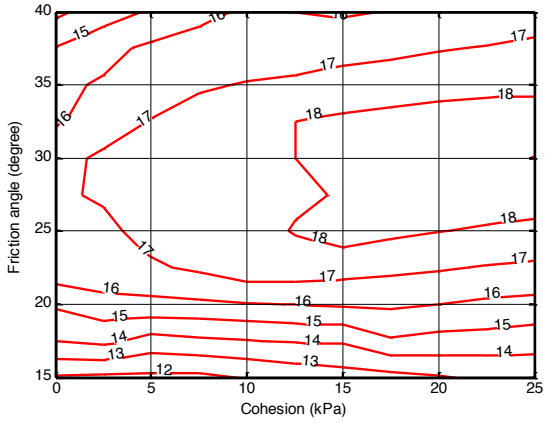

(b) Factor of safety difference when ϕ^b = 15°

Figure 7. Contours of $\Delta F_s/F_{s2D}$ (%) for the steep slope geometry with various shear strength parameters (GWT #2): (a) ϕ^b = 0 (b) ϕ^b = 15°

4 EXAMPLE OF SLOPES WITH TWO INTERSECTING SLOPE SURFACES

A parametric study was conducted on a steep slope with two intersecting slope surfaces (i.e., surfaces forming a concave geometry or a convex geometry). The slope angle was 45 degree. The height of slope was 30 m. The unit weight of the soil was 18.0 kN/m3 and c' was 10 kPa and ϕ' was 34°. The groundwater table was about 5 m below the toe of the slope. The corner angle is defined as the angle between the two intersecting slope surfaces as shown in Figure 8. A slope with a corner angle of 180 degree constitutes a simple geometry slope. A corner angle between 0 and 180 degree is a convex slope. A corner angle ranging between 180 and 360 degrees was defined as a concave geometry slope.

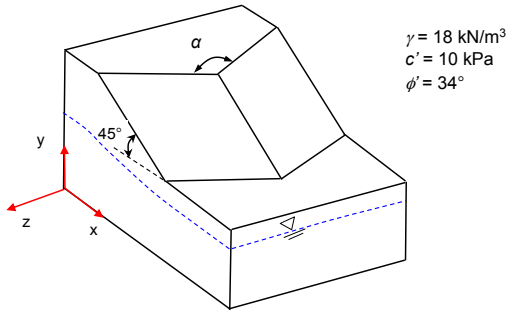

(a) Convex slope geometry

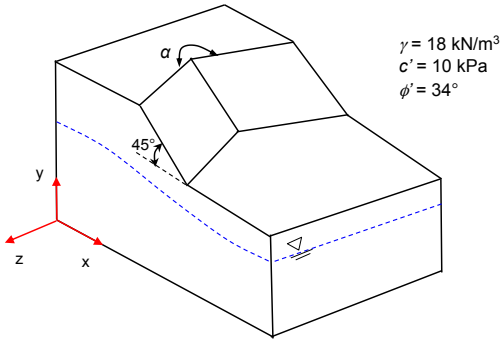

(b) Concave slope geometry

Figure 8. Geometry of steep slopes with two intersecting slope surfaces (a) convex slope geometry (b) concave slope geometry.

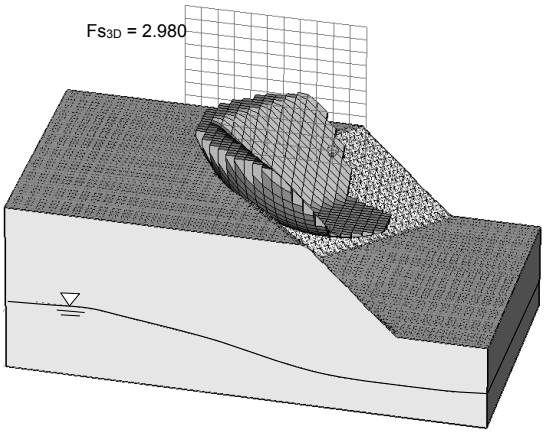

Figure 9. Critical slip surface and failure mass for the concave slope geometry with a corner angle of 270 degree (c' = 10 kPa, ϕ' = 34°, and ϕ^b = 15°).

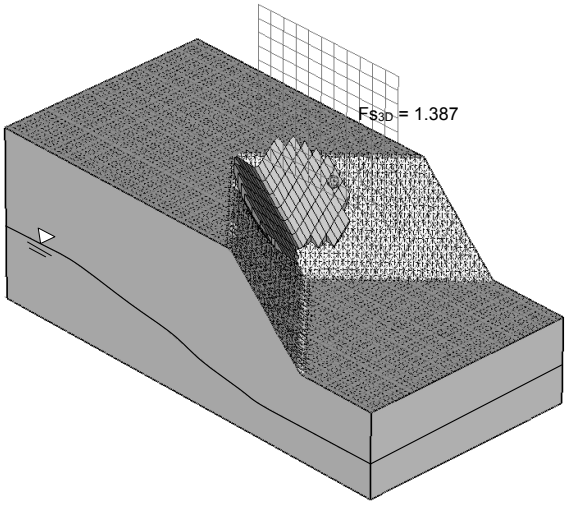

Figure 10. Critical slip surface and failure mass for the concave slope geometry with a corner angle of 270 degree (c' = 10 kPa, ϕ' = 34°, and ϕ^b = 0°).

Figure 9 shows the critical slip surface for a concave slope with a corner angle of 270 degree. The corresponding factor of safety was 2.980. Figure 10 presents the critical slip surface for the convex slope with a corner angle of 270 degree and the omission of matric suction (ϕ^b = 0). The critical slip surface is much shallower than that shown for the concave slope (Figure 9). The calculated factor of safety was 1.387.

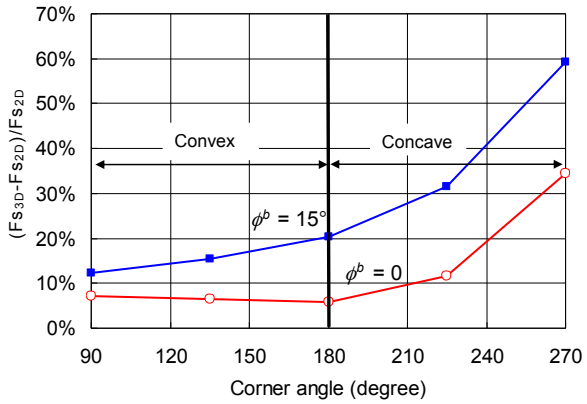

Figure 11. Difference of factor of safety for the steep slope geometry with various corner angles.

Figure 11 illustrates the effect of ϕ^b on $\Delta F_s/F_{s2\text{-}D}$ for slopes with various corner angles. The value of $\Delta F_s/F_{s2\text{-}D}$ is increased substantially with the increase in the ϕ^b value. If ϕ^b is zero, the range of $\Delta F_s/F_{s2\text{-}D}$ varies from 6% to 34% for slope with corner angle ranging from 90 degree (i.e., convex) to 270 degree (i.e., concave). When ϕ^b is 15 degree, the $\Delta F_s/F_{s2\text{-}D}$ ranged from 12% to 59%. The effect of ϕ^b is more pronounced for concave slopes. The range of $\Delta F_s/F_{s2\text{-}D}$ is even smaller than that of simple steep slope for convex slopes.

5 CASE STUDY OF THE POPLAR RIVER MINE HIGHWALL FAILURE

The 2-D and 3-D slope stability analysis was conducted on the case history of the high-wall stability problem at the Poplar River coal mine (Clifton et al., 1986; Lam and Fredlund, 1993).

The Poplar River mine was an open-pit coal mine developed by Saskatchewan Power Corporation to supply coal to the Poplar River Power Station near Coronach, Saskatchewan. A high-wall failure occurred at location TC10 on 22 September 1982. A schematic view showing the geometry of the failed mass along with the inferred position of the slip surface and the approximate position of the external load is illustrated in Fig. 12. The failed high-wall was 15.2 m high with a slope angle of about 33 degrees. The failure occurred along a slicken-sided clay layer approximately 7.6 m below the crest of the high-wall. A layer of wet sand about 1.2 m in thickness was observed above the clay layer. At the time of the failure, the dragline was walking parallel to the high-wall about 20 m away from the crest of the high-wall. The slope failure appeared to be the result of the high stresses exerted by the shoe of the dragline. The external load due to the shoe of the dragline was approximately 215 kPa applied on the slope over an area of 21.9 m by 4.3 m. The distance from the shoe to the crest of the high-wall ranged from 19.5 to 26.0 m.

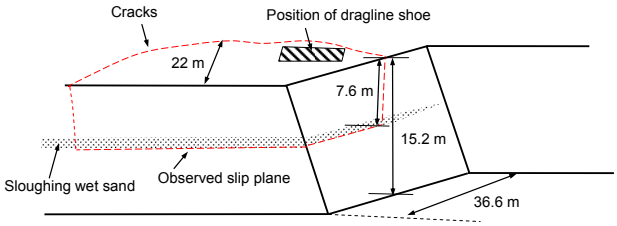

Figure 12. Schematic view of Poplar river mine high-wall failure showing geometry, failure surface and location of external load.

The effective cohesion of and an effective friction angle of internal of the till stratum was 6 kPa and 34°, respectively, based on laboratory test results. According to the laboratory tests (Clifton et al., 1986), the effective cohesion went to zero and the effective friction angle ranged from 11° to 22.8° for the clay stratum at residual conditions.

The slope failure was analyzed using both 2-D and 3-D slope stability analysis. Figure 13 presents the slip surface in the 2-D stability analysis and the failed mass in the 3-D stability analysis. Since no pore-water measurements were obtained at the time of failure, the slope was analyzed as a function of the height of the water table above the slip surface. The residual friction angle for the clay was back-analyzed using the GLE method of analysis satisfying moment and force equilibrium. In the back-analysis, the shear strength of the entire slip surface was assumed to be in the weak clay layer. The unit weight of all the soils was taken to be 19.3 kN/m^3. The back-analyzed residual friction angles of the clay are considerably higher when using a two-dimensional analysis than when using a three-dimensional analysis as shown in Fig. 14. The back-analyzed friction angle for the weak clay layer was over-estimated by around 40% by 2-D analysis.

Two-dimensional and three-dimensional stability analyses were conducted for the condition with the groundwater table being 2 meters below the slip surface. These analyses illustrate the effect of unsaturated zone. The slip surface of the actual failed mass was used. The friction angle of the clay was assumed to be 14°, which was the design value based on the subsequent re-analysis of failures (Clifton et al. 1986). Figure 15 presents the factors of safety with respect to the ratio between ϕ^b and the frictional angle ϕ'. The difference between 2-D and 3-D slope stability analysis is relatively large for this case history. The value of $\Delta F_s/F_{s2\text{-}D}$, ranged from 71% to 90% when ϕ^b increased from 0% to 75% of the effective angle of internal friction, ϕ'.

(a)) 2-D cross-section

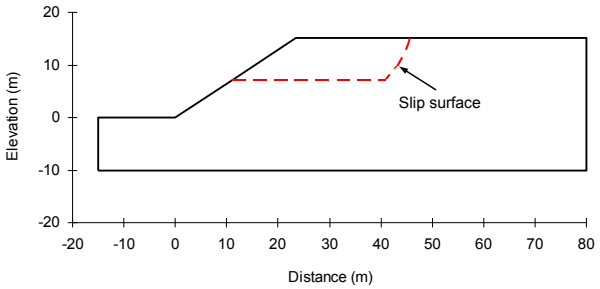

(b) 3-D perspective view

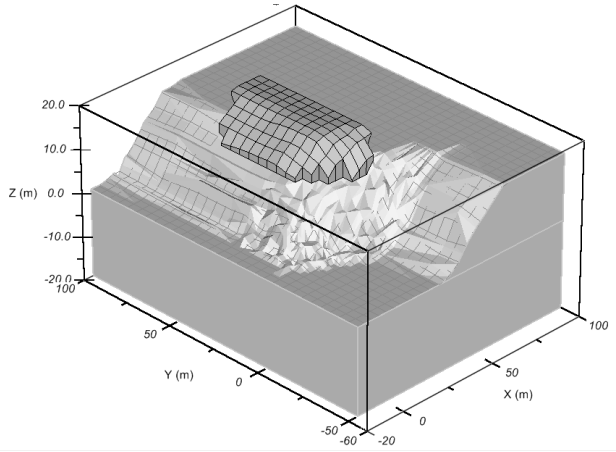

Figure 13. Geometry and failure soil mass of slope stability analysis for Poplar River coal mine high-wall failure.

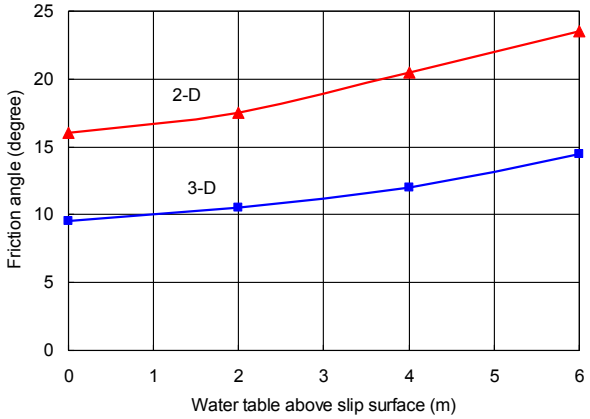

Figure 14. Back-analyzed friction angle of the clay layer for various groundwater table positions.

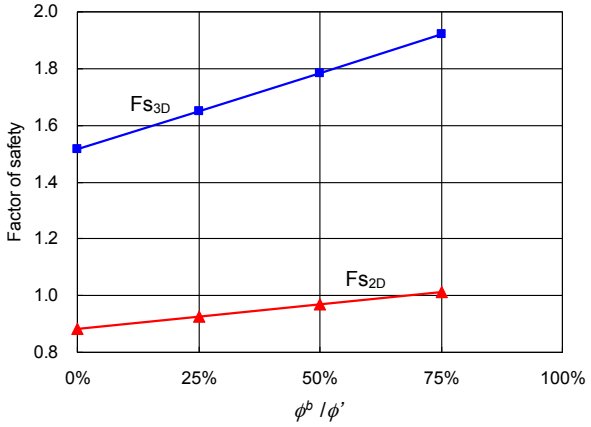

Figure 15. 2-D and 3-D slope stability results considering the effect of the unsaturated zone with the groundwater table 2 m below the slip surface.

Two-dimensional and three-dimensional stability analyses were conducted for the condition with the groundwater table being 2 meters below the slip surface. These analyses illustrate the effect of unsaturated zone. The slip surface of the actual failed mass was used. The friction angle of the clay was assumed to be 14°, which was the design value based on the subsequent re-analysis of failures (Clifton et al. 1986). Figure 15 presents the factors of safety with respect to the ratio between ϕ^b and the frictional angle ϕ'. The difference between 2-D and 3-D slope stability analysis is relatively large for this case history. The value of $\Delta F_s/F_{s2\text{-}D}$, ranged from 71% to 90% when ϕ^b increased from 0% to 75% of the effective angle of internal friction, ϕ' .

6 CONCLUSIONS

A comparative study between 2-D and 3-D slope stability analysis for unsaturated soil slopes is presented in this paper. The major findings can be summarized as follows.

For simple slopes with a low slope angle, $\Delta F_s/F_{s2\text{-}D}$ monotonically increases with an increase in c', ϕ', and ϕ^b values. The variation in $\Delta F_s/F_{s2\text{-}D}$ with various combinations of c' and ϕ' values ranges from 4% to 9% with ϕ^b equal to zero. When ϕ^b is assumed to be 15 degree, the values of $\Delta F_s/F_{s2\text{-}D}$ range from 9% to 16%.

For a simple, steep slope, $\Delta F_s/F_{s2\text{-}D}$ does not increase monotonically with the shear strength parameters (i.e., c', ϕ', and ϕ^b). The difference of factor of safety between 2-D and 3-D analysis for a steep, simple slope is generally larger than that of a low angle, simple slope. When ϕ^b is 15 degree, the values of $\Delta F_s/F_{s2\text{-}D}$ for the simple, steep slope range from 12% to 18% for various combinations of c' and ϕ' values. The effect of groundwater table on the difference between 2-D and 3-D factors of safety is more pronounced for the simple, steep slope than for the low angle slope.

The difference between a 2-D and 3-D stability analysis was most pronounced for concave geometries where a portion of the soil profile contained unsaturated soils. When ϕ^b was equal to 15 degree, the values of $\Delta F_s/F_{s2\text{-}D}$ for concave slopes with a corner angle between 180 to 270 degree can be as great as 20 to 59%.

The back-analyzed shear strength parameters can be significantly over-estimated when using a 2-D stability analysis. For the Poplar mine high-wall failure, the back-analyzed residual friction angle was over-estimated by around 40% when using a 2-D analysis and the value of $\Delta F_s/F_{s2\text{-}D}$, ranges from 71% to 90% when considering the unsaturated zone.

ACKNOWLEDGEMENTS

The work in this paper was substantially supported by the Natural Science Foundation of China (Project No. 41172252) and National Basic Research Program of China (973 Program, Project No. 2014CB049100). The authors are grateful for the supports from the BaJian Talent Program by the Organization Department of the Central Committee of the CPC and the Shanghai Rising-Star Program (Project No. 12QA1401800).

REFERENCES

Adriano, P.R.R., Fernandes, J.H., Gitirana, G.F.N., and Fredlund, M.D. 2008. Influence of ground surface shape and Poisson's ratio on three-dimensional factor of safety. In *Proceedings of GeoEdmonton '08: 61st Canadian Geotechnical Conference Proceedings*, Edmonton, Alberta September 2008.

Chen, R.H., and Chameau, J.L. 1982. Three-dimensional limit equilibrium analysis of slopes. *Geotechnique*, 32(1): 31-40.

Chen, Z.Y., Wang, X.G., Haberfield, C., Yin, J.H., and Wang, Y.J. 2001. A three-dimensional slope stability analysis method using the upper bound theorem. Part I: Theory and methods. *International Journal of Rock Mechanics and Mining Science*s, 38(3): 369–378.

Cheng, Y.M., and Yip, C.J. 2007. Three-Dimensional asymmetrical slope stability analysis extension of Bishop's, Janbu's, and Morgenstern–Price's techniques. *Journal of Geotechnical and Geoenvironmental Engineering*, 133(12): 1544-1555.

Clifton, A.W., Mickleborough, O., and Fredlund, D.G. 1986. Highwall stability analysis under dragline loadings at a Saskatchewan coal mine. In *Proceedings of the Symposium on Geotechnical Stability In Surface Mining*, Calgary, Alta., pp. 341-353.

Duncan, J. 1996. State of the art: limit equilibrium and finite-element analysis of slopes. *ASCE Journal of Geotechnical Engineering*, 122(7), 577-596.

Fredlund, D.G., and Krahn, J. 1977. Comparison of slope stability methods of analysis. *Canadian Geotechnical Journal*, 14(3): 429-439.

Fredlund, D.G., Rahardjo, H., and Fredlund, M.D. 2012a. *Unsaturated Soil Mechanics in Engineering Practice*. John Wiley & Sons. New York, N.Y., 926 p.

Fredlund, M.D. 2009. *SVSlope User's Manual*. SoilVision System Ltd, Saskatoon, Canada.

Fredlund, M.D., Lu, H., Fredlund, D.G. 2012b. Benchmarking of a three-dimensional limit equilibrium slope stability software. In *Proceedings of GeoManitoba*, Winnipeg, MN, Canada, September 30 - October 3, 2012.

Hovland, H.J. 1977. Three-dimensional slope stability analysis method. *ASCE Journal of the Geotechnical Engineering Division*, 103(GT9): 971-986.

Hungr, O. 1987. An extension of Bishop's simplified method of slope stability analysis to three dimensions. *Geotechnique*. 37(1): 113-117.

Kalatehjari, R. and Ali, N. 2013. A review of three-dimensional slope stability analyses based on limit equilibrium method, *The Electronic Journal of Geotechnical Engineering*, 2013(18/A): 119-134.

Lam, L. and Fredlund, D.G. 1993. A general limit equilibrium model for three-dimensional slope stability analysis, *Canadian Geotechnical Journal*, 30(6): 905-919.

Leong, E.C., and Rahardjo, H. 2012. Two and three-dimensional slope stability reanalyses of Bukit Batok slope. *Computers and Geotechnics*, 42: 81-88.

Leshchinsky, D., and Baker R. 1986. Three-dimensional slope stability: end effects. *Soils and Foundations*, 26(4): 98-110.

Leshchinsky, D. and Huang, C. 1992. Generalized three dimensional slope stability Analysis. *ASCE Journal of Geotechnical Engineering*, 118(11): 1748–1764.

Morgenstern, N.R., and Price, V.E. 1965. The analysis of the stability of general slip surfaces. *Geotechnique*, 15(1): 79-93.

Stark, T.D., and Eid, H.T. 1998. Performance of three-dimensional slope stability methods in practice. *Journal of Geotechnical and Geoenvironmental Engineering*, 124(11): 1049-1060.

Yu, Y., Xie, L., and Zhang, B. 2005. Stability of earth–rockfill dams: influence of geometry on the three-dimensional effect. *Computers and Geotechnics*, 32(5), 326-339.

Zhang, X. 1988. Three-dimensional stability analysis of concave slopes in plan view. *ASCE Journal of Geotechnical Engineering*. 114: 658-671.

Zheng, H. 2012. A three-dimensional rigorous method for stability analysis of landslides. *Engineering Geology*. 145: 30-40.